

THE DEVELOPMENT OF THE THIRD GENERATION WAVE MODEL MRI-III FOR OPERATIONAL USE.

Koji Ueno¹ and Nadao Kohno²

¹Meteorological College
¹Asahi-cyo, Kashiwa-shi, Chiba, Japan

²Meteorological Research Institute
²Nagamine Tsukuba-shi, Ibaraki, Japan

1. INTRODUCTION

There have been developed several third generation wave models since the pioneering work of the WAM model (WAMDIG 1988). The WAM is the first model which calculates explicitly nonlinear energy transfers by resonant wave-wave interaction, and used for operational ocean wave predictions. Following this success, several wave models were developed, and the WAM itself is also improved to the cycle 4 version and used in various fields.

All of these models use the DIA scheme by Haselmann et al. (1985) in calculation of the nonlinear energy transfer, since the DIA scheme is the first and almost only one practical method. On the contrary, rigorous calculation of the nonlinear energy transfer are also carried out and used in researches, but elapsed time is too long for operational works.

The DIA scheme considers only one configuration of resonant four-waves. This method estimates proper energy transfer value to the lower frequency side, but also calculates a spurious energy transfer toward the higher frequency range.

To improve this problem the DIA scheme is modified. The new scheme uses three configurations of the resonant four waves. Hereafter we refer this scheme to the extended DIA (EDIA). The EDIA scheme has three advantages:

- a. The estimated S_{nl} profile is almost same as rigorous one in various spectra -the PM-spectrum, the JONSWAP-spectrum, etc. (We tuned coefficients as the EDIA estimates the same peak value as exact calculation in case of a JONSWAP-spectrum, and this leads to 1.7 times larger in case of the PM-spectrum though original DIA estimates 4 times larger values.)
- b. The spurious energy transfer does not occur.
- c. The calculation time is much shorter than the rigorous calculation.

But this causes the over-estimation of wave heights of swell. From our research, this problem results from the nonlinear energy transfer S_{nl} , not the energy dissipation S_{ds} . The cause is the EDIA scheme itself, since the MRI-III predicts proper swell if S_{nl}

term is just replaced to the DIA scheme.

Therefore, a new source function for swell decay is introduced.

In the MRI-III, major improvements are two points:

- (1)The EDIA scheme is used in non-linear energy transfer calculation, which leads to closer estimation of S_{nl} to the exact values.
- (2)The swell decay term was newly introduced in order to clear the problem of over-estimation.

2. MODEL DESCRIPTION

A component of two-dimensional spectrum of waves at any place and time (x,y,t) is expressed as $F(x,y,t,f,\theta)$ in frequency f and wave direction θ . The governing equation is

$$\frac{\partial F(x,y,t,f,\theta)}{\partial t} + \nabla \cdot C_g(f) \cdot F(f,\theta) = S_{in} + S_{nl} + S_{ds} \quad (1)$$

which is referred to as the energy balance equation. The second left term is advection term and expresses swell propagation. S_{in} , S_{nl} and S_{ds} are the source terms which express energy input from wind, non-linear energy transfer and energy dissipation respectively.

2.1 Energy Input from Wind S_{in}

The energy input from wind S_{in} is expressed as the form of $S_{in} = A + BF$, where A shows linear wave growth and BF exponential growth. As A term expression, we adopt the expression of Cavaleri and Malanotte-Rizzoli (1981);

$$A = \frac{1.5 \times 10^{-3} u_*^4}{g^2 2\pi} \exp\left[-\left(\frac{\sigma}{\sigma_{PM}}\right)^4\right] \cdot \{u_* \cdot \max(0, \cos\theta - \theta_w)\}^4 \quad (2)$$

where θ is the direction of component waves, u_* the friction velocity of wind, θ_w the wind direction, g the gravitational acceleration. In general, this term has little influence on wave growth except very early stage, we may omit this term if only moderate wave conditions are concerned.

On the other hand, the exponential term BF has the principle role in wave growth, and then the coefficient B has critical importance. In the MRI-III,

the expression by Plant (1982) or Mitsuyasu and Honda (1982) is used since this formula is adaptable in wide range of wave age from laboratory to ocean.

$$B = 0.32 \frac{\cos(\theta_w - \theta)}{|\cos(\theta_w - \theta)|} \left(\frac{u_*}{C_p} \right)^2 \cos^2(\theta_w - \theta) \quad (3)$$

2.2 Nonlinear Energy Transfer S_{nl}

The rigorous calculation of nonlinear energy transfer needs triple integration over wave number space for one component and consumes too much time. Therefore, the rigorous calculation is not available in operational wave models. Hasselmann et al. (1985) proposed a practical scheme referred to as the Discrete Interaction Approximation (DIA) as,

$$\begin{aligned} f_1 &= f_2 = f, \\ f_3 &= f(1 + \lambda) = f_+, \\ f_4 &= f(1 - \lambda) = f_- \end{aligned} \quad (4)$$

$$\begin{aligned} \begin{Bmatrix} S_{nl} \\ S_{nl}^+ \\ S_{nl}^- \end{Bmatrix} &= \begin{Bmatrix} -2 \\ (1 + \lambda) \frac{\Delta\omega \Delta\theta}{\Delta\omega_+ \Delta\theta} \\ (1 - \lambda) \frac{\Delta\omega \Delta\theta}{\Delta\omega_- \Delta\theta} \end{Bmatrix} \cdot C \frac{f^{11}}{g^4} \\ &\cdot \left[F^2 \left\{ \frac{F_+}{(1 + \lambda)^4} + \frac{F_-}{(1 - \lambda)^4} \right\} - 2 \frac{FF_+ F_-}{(1 - \lambda^2)^4} \right] \end{aligned} \quad (5)$$

where $F = F(f, \theta)$, $F_+ = F(f_+, \theta_3)$, $F_- = F(f_-, \theta_4)$. The coefficient C is determined to be fitted to the exact calculation. Hasselmann et al. (1985) determined the parameters as $\lambda = 0.25$ and $C = 3 \times 10^7$.

However, this parameter produces inconsistency between the DIA and the exact calculation:

- Nonlinear energy transfer for the PM spectrum calculated with the DIA is about four times larger than the exact calculation.
- The DIA produces a strong negative lobe and a positive lobe at $1.6f_p$ as shown in Fig. 1.

In Fig. 1 one-dimensional energy transfer S_{nl} is plotted versus the dimensionless angular frequency. These values are also expressed by non-dimensional values multiplied by $F(f_p)^3 \omega^{11} g^{-4}$. The directional distribution of the two-dimensional spectrum is supposed to be $\cos^2 \theta$ irrespective of frequency. The exact calculations denoted by the solid line were carried out by Dr. Komatsu and Prof. Masuda. The DIA is shown by the broken line. In case of the PM-spectrum, the S_{nl} profile itself is similar to exact one

in quality, though the peak value is much larger than the exact one. However, in case of the JONSWAP-spectrum and a more narrow spectrum (e.g. the peak enhancement factor $\gamma = 5.0$), nor the extreme values and nor the profile agree with the exact calculation, even though the value of energy transfer toward lower frequency side, which may has a significant role on wave evolution, are consistent.

In order to make a drastic improvement of the approximation of the nonlinear energy transfer, the MRI-III uses the three configurations of the resonant four waves. The parameters are set as $\lambda_1 = 0.19$, $C_1 = 1.19^7$, $\lambda_2 = 0.23$, $C_2 = 6.84^6$, and $\lambda_3 = 0.33$, $C_3 = 1.63^6$, that lead to fair approximation as shown in Fig. 1. The SRIAM uses twenty configurations of four waves in nonlinear calculation and has the almost same accuracy as exact calculation (Komatsu and Masuda, 2000), though this scheme need much computing time and it may not be yet to be used in operational works.

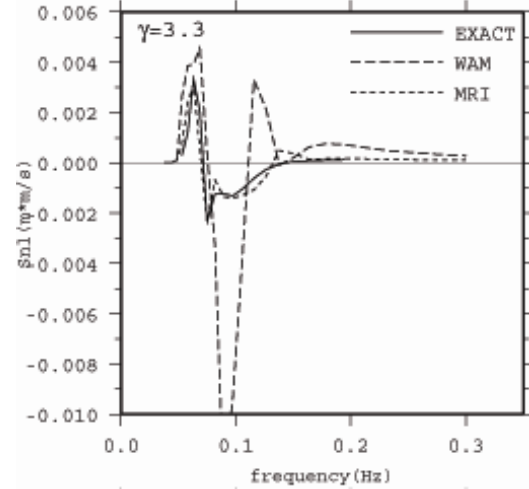


Fig.1 One-dimensional nonlinear energy transfer in case of JONSWAP spectrum.

2.3 Energy Dissipation S_{ds}

The energy dissipation term is newly determined in the MRI-III. In a stationary condition, three conditions are supposed to be maintained in higher frequency area than peak frequency:

$$\begin{aligned} (1) S_{in} &\propto \left(\frac{u_*}{C_p} \right)^2 f \cdot \cos^2 \theta \cdot F(f, \theta) \\ (2) S_{in} &\approx S_{ds} \\ (3) F(f, \theta) &\propto g u_* f^{-4} \cos^2 \theta \end{aligned} \quad (6)$$

Each proposition is derived as follows. The first proposition just comes from the equation (3). The second proposition derived from the supposition

that S_{nl} is small in high frequency range where wave energy is widely spreading and the contrast between components is small. The third proposition is based on the equilibrium of spectrum in high frequency proposed by Toba(1973) and with the product of directional function $\cos^2\theta$.

From these propositions the relation of,

$$S_{ds} = -c_b \frac{u_*}{g^3} f^7 \cdot F(f, \theta)^2 \quad (7)$$

is derived. Here c_b is a coefficient and determined to fit with wave generation. Ueno(1998) explained how to derive these formulae in detail.

We also introduced the swell dissipation explicitly, though it is hypothetical. Let the peak frequency f_p being determined from the 10m height wind speed, wave energy is reduced in the part where frequency is smaller than $f_s = 0.5 f_p$ with a rate of

$$S_{sds} = -4.01 \times 10^{-6} \tanh \frac{f_s - f}{f_p} F(f, \theta) \quad (8)$$

which corresponds to swell decay of $\exp(-4.01 \times 10^{-6} \times 86400) = 0.71$ per day (86400 sec.). Since swell tends to have its energy in lower frequency side than windsea, energy spectra in apparently lower frequency part than the peak frequency of windsea are automatically reduced. The reason of this additional decay is to modify the overestimation of swell. Though it was supposed at first to be the problem of expression of S_{ds} in MRI-III, which is proportional to f^7 and becomes weaker in low frequency area, the overestimation is not cleared if this term is changed to WAM type (Komen et al., 1984). The overestimation may not come from the problem of expression of S_{ds} , but from another one: This comes from the exact S_{nl} estimation according to our research, which means it is reasonable, not mistake. Therefore it may be necessary to introduce additional scheme to decay swell. The reason why nonlinear energy transfer effects to swell decay is mentioned in discussion.

This expression and its value is not yet certain, but at least now, supposed to be reasonable.

2.4 Supplemental numerical treatment

The MRI-III is defined on spherical coordinate with geophysical linear grids. The two-dimensional spectra F have 25 components in frequency, 16 components in direction, and total wave spectra consists of 400 components. The frequencies of spectral components are spaced logarithmically from the minimum of $f_{min} = 0.0375\text{Hz}$ (26.67sec.) to the

maximum of $f_{max} = 0.3000\text{Hz}$ (corresponding wave period is 3.33 sec.), and the wave directions of spectral components are divided linearly.

The directional components are defined at the middle point of directional fragments ('staggered' points) shown as Fig.2. The reason of this definition is connected with advection term.

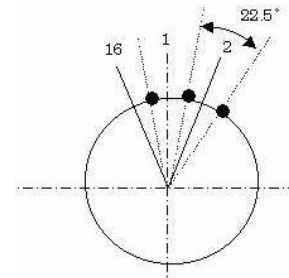


Fig.2 Directional distribution in definition. Directional spectra are defined on the center of directional ranges (staggered points).

We use the simple first order upstream scheme. This scheme is simple and requires only short time for calculation, and also has an advantage of conservation of total energy and generating no negative values from truncation errors, which is desirable to wave energy spectra, since energy spectrum is defined as positive value. A demerit of this scheme is numerical diffusion, though this 'sprinkler effect' is rather convenient for wave model of so far as angular dispersion is concerned.

However, this scheme has demerit of anisotropic dispersion. For example, wave spectral component propagating from due north / south or east / west loses its diffusiveness (e.g. Fig.1 of The WAMDI group (1988)) since the values of cosine or sine in group velocities defined in spherical plain become zero. However, it is not reasonable to the spectral component with a definite directional width. In order to avoid the anisotropic dispersion we distribute directional components at 'staggered' direction shown as Fig.2.

3. BASIC PERFORMANCE

In order to check the basic performance of the MRI-III, ideal wave generation of the test case 2 in the SWAMP program (The SWAMP Group, 1985) is performed. To examine the growth rate in detail, we compared the growth curve of the MRI-III with

several major ones. The growth curves compared here are those of (1) Wilson (1965), (2) JONSWAP (Hasselmann et al., 1973), (3) Mitsuyasu (1968) and (4) Toba (1978) shown as Fig. 3.

Ebuchi (1999) investigated the one-dimensional fetch growth of wind waves in the Japan Sea using the satellite data and concluded that the growth rate fits with the Toba formula (1978) and is close to the Wilson formula (1965). This result comes from the fetch length since the Japan Sea has long fetch and Wilson and Toba formula are derived from the ocean data. Since the JONSWAP and the Mitsuyasu curve are defined only in the short fetch range ($X^* < 10^{5-6}$), this discrepancy may be reasonable.

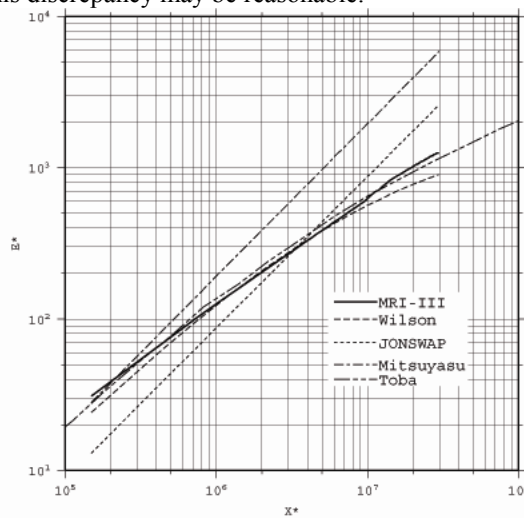


Fig.3 Growth rate in fetch limited condition

The growth rate Ebuchi (1999) examined is worth comparing our ideal growth result since the Japan Sea is almost closed sea and wave start growing with static state under constant strong wind. The growth rate of the MRI-III shown in Fig. 2 also fits well with Wilson and Toba formula and the growth curve of the MRI-III is just between them and its rate is quite resembled to these formulae, but smaller than the JONSWAP and the Mitsuyasu rate.

From these results the growth rate of the MRI-III should be satisfactory.

4. THE HINDCAST IN REALISTIC SEA

The realistic simulations using the MRI-III were performed. We show here the global calculations. The global calculation was carried out in full domain except pole areas, though our concern is restricted only in the Pacific Ocean. The calculated

results are compared with buoy observations in the northwestern Pacific. The computational domain is set as 70.0 deg. -70.0 deg. in latitude, whole in longitude (cyclic) and the grid resolution is set as 2.5 degrees both in lateral and longitudinal directions. The simulated term is the one month of January 2000, but swell has significant role in a wide ocean and calculation started from December 1, 1999 and 1 month is spent for swell spin up. The meteorological input was derived from the 6 hourly JMA global analysis data (GANAL). The way of replace of wind fields is same as the previous regional case. There are 14 buoys in the northwestern Pacific, 3 are deployed by JMA and the others by NOAA.

As for wave condition in the northwestern Pacific during winter season, we may summarize three major characters: Around the Japan, winter monsoon bursts frequently generate windseas, but whose periods do not become so long since wind bursts cease within a few days. On the contrary, fully developed windseas tend to be generated by strong winds of developed polar lows which tend to be stationary in the Aleutian Sea. These high windseas tend to propagate toward the sea off Hawaii as high sells. Since meteorological disturbance like hurricane seldom generate winter season around Hawaii, swell are predominant in the sea off Hawaii. In this calculation whether these three situations are properly simulated or not, are concerned.

At first, the wave condition around the Japan was checked, since the performance of the Japan Sea has already been checked previous section. The time sequences of wave heights at the buoy points around Japan are shown as Fig. 4.

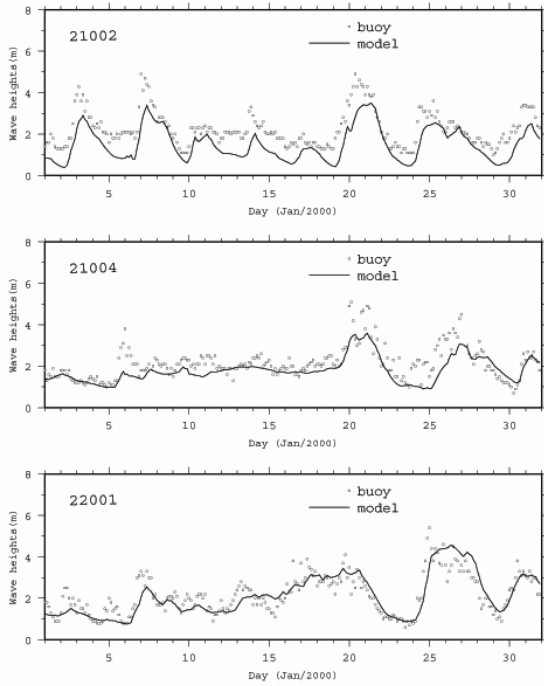


Fig.4 Comparison of model results with buoy data around Japan (wave heights).

Compared with tree buoys - the Japan Sea (21002), the East China Sea (21004) and the Sea off Shikoku (22001), both the wave heights and periods are well estimated except in the Japan Sea. Though there are some miss estimation as the day of 6, 24 and 25 at the East China Sea and 7 at the Sea off Shikoku, the extreme events on 21 at the East China Sea and 20, 25 and 31 at the sea off Shikoku are well estimated. The wave decay is also properly estimated in both areas.

However the under estimation in the Japan Sea is noticeable. The reason why wave values are underestimated in the Japan Sea may be due to 2 factors: One is the problem of the surface wind. The surface wind speed at the buoy of 21002 is systematically weak, especially in high wind events. (The model winds have almost 1.0m/s lower bias and much weaker in their peak values.) This lack of energy input from winds must be main reason for underestimation. In this global calculation we did not consider the adjustment in stability change since we have not had full information about it in global area. This may be also the reason of underestimation, as mentioned in previous section.

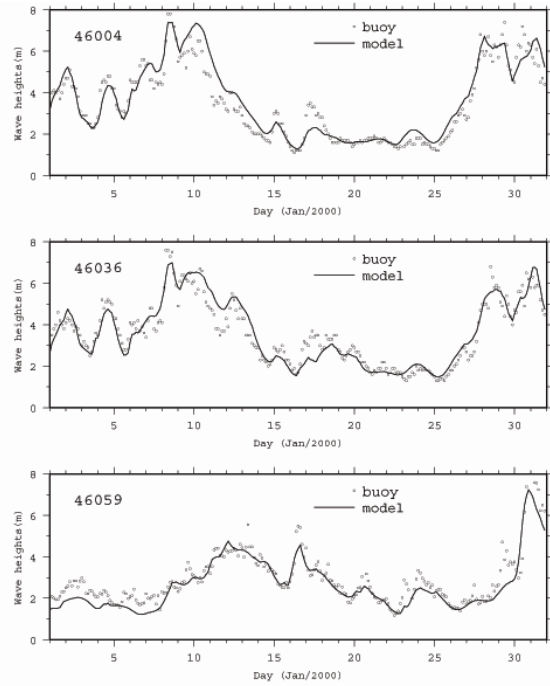


Fig.5 Comparison of model results with buoy data in Aleutian Sea (wave heights).

The other is the problem of grid resolution. The grid resolution of 2.5 degree is very coarse for the Japan Sea because the Japan Sea consists of only ten and a few grids. Considering these reasons, the underestimation at the Japan Sea may not come from the model physics itself, and we may expect that the MRI-III has an ability of good estimation if good environmental condition is given.

Fig.5 shows the waves in the Aleutian Sea. The estimated values by the MRI-III are quite accurate compared with buoy data. Not only high wave events of over 6m (the day of 8, 10 and 28-31 at 46004 and 46036, 31 at 46059) but also moderate wave condition of 2-3m, the MRI-III correctly estimated. The tendency of wave heights is quite consistent with buoy data. The correlations between model and observations are over 0.94. The wave period tends to be underestimated, its values are reasonable in general. The products of wave period of NOAA buoys are defined as discrete values in their long values, and the difference from the simulation may come from this systematic problem. Anyway the qualitative tendency of simulation is quite agree with the observation. Therefore the MRI-III can estimate reasonable windsea evolution and decay.

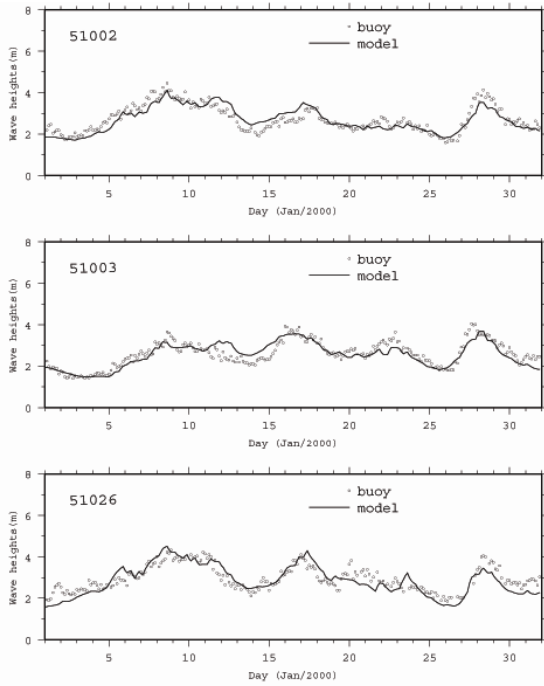


Fig.6 Comparison of model results with buoy data off Hawaii (wave heights).

The calculated wave states in the Sea off Hawaii are shown in Fig.6. These wave are supposed to be swell and swell heights are quite good agreement with observations, which may be partly because we could simulate proper windseas in the Aleutian Sea, since windsea there is the main source of sell. The swell decay term is explicitly included in our model, and at least the estimated values are concerned, this term may be regarded as reasonable.

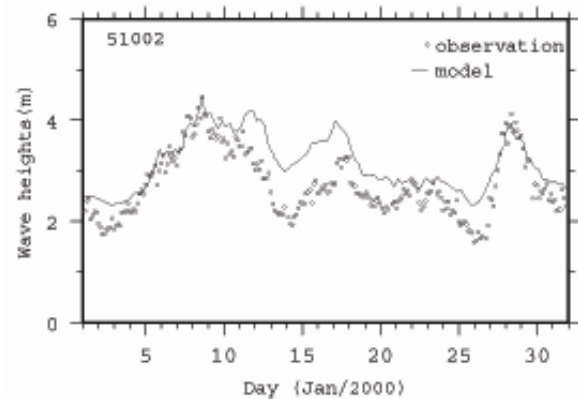
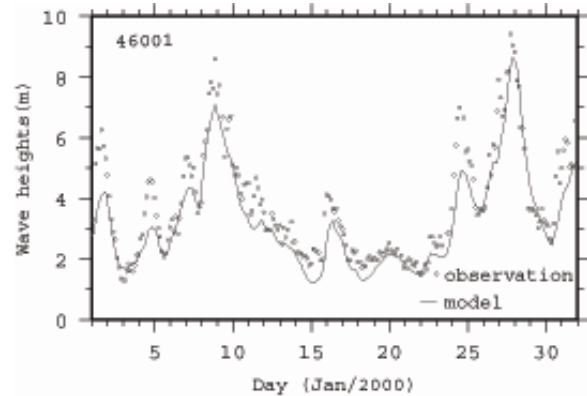
However there are still miss-simulated parts in our calculation. These misleading may come from errs of the wind fields. Though the general features of wind condition is in good agreements, the peak values of model wind are sometimes weaker than those of observations and wind scatters measured in buoys are not well expressed in model winds. The wind speeds correlations are ranged between 0.77 and 0.91, except 0.61 of 46061 buoy at Aleutian. The 46061 buoy is located in near land grid and may be influenced it. In general, the correlations of wind are slight lower than that of wave heights. This suggests that the wave model can estimate closer tendency than winds since wave state is not change so quickly as wind field.

5. DISCUSSION

We will further discuss about the feasibility of

the expression of source terms used in the MRI-III, especially 1) the effect of the EDIA scheme and the influence of nonlinear energy transfer to wave energy dissipation, 2) the reasonability of new dissipation term and 3) the role of swell decay term newly introduced. To examine them, we carried out another 2 calculations:

- A. the EDIA scheme is holds in S_{nl} but the swell decay term is not included,
- B. the DIA scheme is used in the S_{nl} and the swell decay term is not included.



(1)

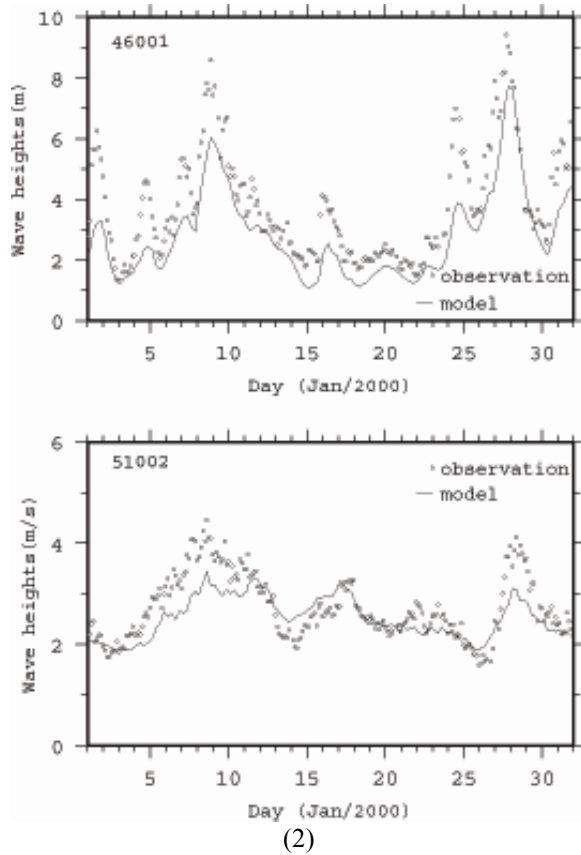


Fig.7 The difference of wave height of (a)46001 and (b)51002 in case of A(1) and B(2). The dots and lines show the observation and calculation respectively. The buoy of 46001 expresses the wind sea height, and 51002 buoy swell height.

The terms S_{in} and S_{ds} keep same as the control run in both calculations. Fig. 7 (a)□(b) show the sequences of wave heights in the Aleutian (46001) and the Sea off Hawaii (51002) in the case of A and B.

The EDIA scheme estimate much accurate nonlinear values than the DIA scheme used in the WAM, and this may lead to proper estimation in development of high windseas. The test calculation shows that the EDIA scheme could estimate much accurate peak values than the DIA scheme in the Aleutian Sea. Though general tendency and wave decay is almost same in both calculations, the peak values of wave height by the DIA scheme apparently are underestimated.

On the contrary, the swell heights in the Sea off Hawaii are rather overestimated by the EDIA, though the DIA scheme looks like properly estimates the swell. This may be partly because that underestimation of windsea prevents from overestimation of swell heights in the case B, but it is

not reasonable even if swell is correct. The both calculations have the same correlation values as 0.84, and then the tendency is same but the value is different. The EDIA scheme estimates much accurate windseas and swell tendency though only swell heights are overestimated.

What makes this overestimation? To tell the truth, we at first suspect the feasibility of the S_{ds} expression by Ueno (1998), and replace this term to that of Komen et al.(1984) used in the WAM. The results turned out to be no significant difference in both calculations, and we conclude that the S_{ds} expression by Ueno (1998) may be as reliable as other expression used in other wave models.

Since both S_{in} and S_{ds} terms have no connection with this problem, this must come from S_{nl} term. But there is no energy addition or subtraction in nonlinear energy transfer. According to Fig.1, when spectral density is not widely spread, as is the often case of swell, the DIA scheme also transfers much energy to higher frequency side, not only lower side. Since the exact calculation does not transfer such large energy toward higher frequency side, the DIA scheme spuriously transfers the wave energy toward higher frequency region.

In general, wave energy dissipation is predominant in their high frequency region, S_{ds} term is expressed as to be larger dissipation of wave energy in high frequencies. This character is same in both the expression of Ueno (1998) and Komen et al. (1984) used in the WAM. Therefore, the energy transferred to higher frequency side is effectively dissipated and this leads to larger energy dissipation. The problem is that the additional dissipation in high frequency region comes from spurious nonlinear energy transfer.

In order to check the swell dissipation itself, swell propagation test was carried out. Fig. 8 shows the time sequence of the peak wave height during 30 days under wind speed of 5m/s. The initial wave energy is JONSWAP spectra of 20m/s wind, and then this wave should be regarded as perfectly swell in all time. In the case of A, the wave height 30 days later is still about 2m, which is much larger value considering the wind condition of 5m/s wind. The wave period is also as large as over 12 second. In the case of B, swell decayed to reasonable values as wave height of about 1m, and the peak period is also shorten to 9 second.

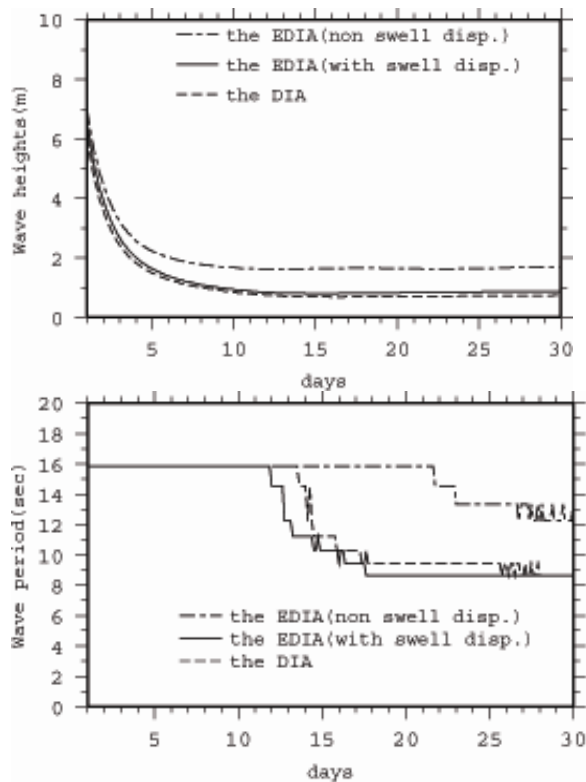


Fig.8 The swell decay during 30 days under 5m/s wind. Wave heights(upper) and period(lower). The broken line shows the calculation with the DIA scheme and dot chain line shows the result with the EDIA scheme, and swell decay term was not included in both calculations. The full line shows the calculation with the EDIA scheme and swell decay term.

From these results, the DIA scheme looks like to estimate good swell decay. However, even if the DIA scheme estimates good swell heights, such values comes from spurious transfer and not preferable. Since the EDIA scheme tends to over estimate swell heights due to accurate nonlinear energy transfer, it is supposed to look for new mechanism of swell decay. Therefore we introduce swell decay term though it is slight artificial. This is because that we have not plenty of knowledge about swell decay, and we must rely on the empirical method to fit with observations.

This new modification for swell decay looks like functions well. The swell heights estimated by the MRI-III become similar to the values in the case of B and reasonable. This new term has another advantage. Since we divide the term of wind sea growth and swell decay, we are able to optimize these coefficients independently and expect good estimation of both windseas and swell.

6. CONCLUSION

The third generation wave model MRI-III for operational use has been developed. In this model, nonlinear energy transfer is estimated by the EDIA scheme, which multiples the configuration parameter in the DIA scheme used in the WAM etc. The EDIA scheme has much precision than the DIA scheme and ability of estimating almost same values as the exact calculation. Although the EDIA scheme needs much time than the original DIA, it is just a few times and enough to be adaptable for practical use.

The new scheme happened to have a new problem that swell energy becomes larger values than the case by the DIA. Having checked this problem, the DIA scheme transfers wave energy toward the higher frequency side, which plays a significant role in decreasing swell energy, but it is not the case in exact calculation.

There is no such spurious energy transfer in the EDIA, but it leads to over estimation of swell. Therefore, swell decay term has been newly introduced in the MRI-III and the MRI-III comes to have high accuracies both in windsea and swell. The simulation in realistic seas (the Japan Sea and the global ocean) results in quite good estimation.

The expression of the swell decay term is hypothetical, and then we need further research to detect the mechanism of swell decay and develop the expression this term.

REFERENCE

- Cavaleri L. and P. M. Rizzoli (1981): Wind wave prediction in shallow water: theory and applications. *J. Geophys. Res.*, 86, 10961-10973.
- Ebuchi, N. (1999):Growth of wind waves with fetch in the Sea of Japan under winter monsoon investigated using data from satellite altimeters and scatterometer. *J. Oceanogr. Soc. Japan.*, 55, 575-584.
- Hasselmann, K., T. P. Barnett, E. Bouws, H. Carlson, D. E. Cartwright, K. Enke, J. A. Ewing, H. Gienapp, D. E. Hasselmann, P. Kruseman, A. Meerburg, P. Mullar, D. J. Olbers, K. Richter, W. Sell and H. Walden (1973): Measurement of wind-wave growth and swell decay during the joint North Sea Wave project (JONSWAP). *Dtsch. Hydrogr. Z.*, 8 (12), suppl. A., 95pp.
- Hasselmann, S., K. Hasselmann, J. H. Allender and T. P. Barnett (1985): Computations and parameterizations of the nonlinear energy transfer in a gravity-wave spectrum. Part II: Parameterizations of the nonlinear energy transfer for application in wave models. *J. Phys. Oceanogr.*, 15, 1378-1391.
- Komen, G. J., K. Hasselmann and S. Hasselmann (1984): On the existence of a fully developed windsea spectrum. *J. Phys. Oceanogr.*, 14, 1271-1285.

Mitsuyasu, H (1968): On the growth of the spectrum of wind generated waves (1). Rep. Res. Inst. Appl. Mech., Kyushu Univ., 16, 459-482.

Mitsuyasu, H. and T. Honda (1982): Wind-induced growth of water waves. J. Fluid Mech., 123, 425-442.

Plant, W. J. (1982): A Relationship between wind stress and wave slope. J. Geophys. Res., 87, 1961-1967.

Toba, Y. (1973): Local balance in the air-sea boundary processes III. On the spectrum of wind waves. J. Oceanogr. Soc. Japan., 29, 209-220.

Toba, Y. (1978): Stochastic form of the growth of wind waves in a single-parameter representation with physical implications. J. Phys. Oceanogr., 8, 494-507.

Tolman, H. L. (1992): Effects of numerics on the physics in a third-generation wind-wave model. J. Phys. Oceanogr., 22, 1095-1111.

The SWAMP Group (1985): Ocean Wave modeling. Plenum, 256pp.

The WAMDI Group (13 Authors) (1988): The WAM model - A third generation ocean wave prediction model. J. Phys. Oceanogr., 18, 1775-1810.

Ueno, K. (1998): On the energy dissipation term of wave models. Sokkou-Jihou, 65, S181-S187. (in Japanese)

Wilson, B. W. (1965): Numerical prediction of ocean waves in the North Atlantic for December 1959. Dtsch. Hydrogr. Z., 18, 114-130.